Probing the dimensions of semi-rigid inner functionalised U-shaped *bis*-porphyrin cavities

Shaun P. Gaynor,[a] Maxwell J. Gunter,*[a] Martin R. Johnston[b] and Ronald N. Warrener[c]

Received 30th January 2006, Accepted 5th April 2006
First published as an Advance Article on the web 4th May 2006
DOI: 10.1039/b601417h

The synthesis of a series of open U-shaped *bis*-porphyrin cavity molecules is described, with bridged bicyclic backbones to confer rigidity, and a pendant substituted aromatic probe unit suspended on the inside of the cavity. The dimensions and flexibility of the *bis*-zincporphyrin cavity were probed using several different techniques. Initially the molecular ruler concept was employed, using flexible bidentate ligands as guests with a range of possible linear dimensions. Secondly, NMR methods were employed with rigid bidentate ligand guests of fixed lengths, and thirdly diffusion based NMR methods were utilised. The range of inter-porphyrin distances estimated by these methods suggests that these types of open-cavity systems have a surprising degree of flexibility.

Introduction

The design and construction of electronic devices that operate at a molecular level are fundamental tenets of molecular engineering.[1,2] This necessarily requires the production of molecular and supramolecular assemblies which are able to operate as molecular analogues of macroscale electronic components and circuitry, and which can be utilised in the ultimate construction of organised functional nanostructures. For example, the principles of molecular relays, switches, diodes, and logic devices utilising the concept of mechanical movement of the component parts of particular supramolecular systems are being actively pursued, although there is some question as to whether these state changes will be rapid enough for the fast switching required for the next generation of electronic componentry.[3,4] These systems often involve assemblies such as (pseudo)rotaxanes, catenanes, or association complexes with in-built addressable functionality to control mechanical movement of various parts of the assembly.[2,3,5]

We have developed an approach which incorporates a rigid U-shaped cavity holding a pair of rigidly fused porphyrin units, and a relay component which is free to move conformationally relative to the cavity (Fig. 1a). This central component provides a tethered electron relay unit which can potentially carry a signal from one side of the system to the other, the two units being otherwise isolated by an electrically insulating connection. These systems have the potential to function as photo- or electro-active switches, relays, diodes or logic gates. Similar arrangements have also been used to probe the dynamics of electron and energy transfer to delineate through-bond and through-solvent contributions, mediated in some instances by the intervening tether unit.[6,7]

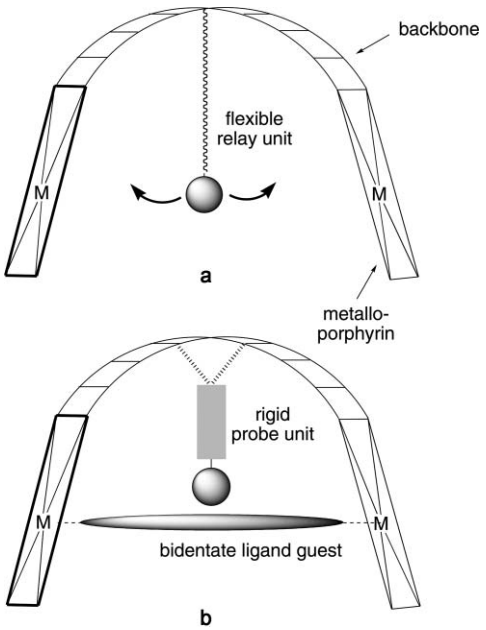

Fig. 1 Cartoon of the arrangement of the units in the porphyrin–spacer–porphyrin (PSP) assemblies used in previous work (a) and this work (b).

Other related semi-rigid U-shaped porphyrinic structures which are based on a similar architecture (as in Fig. 1a, but lacking the flexible relay unit) have been studied for a variety of different functions, including molecular capsules,[8,9] a molecular scale 'universal joint',[10] as receptors for photoactive substrates[11–13] and as possible catalytic systems for intermolecular reactions[14,15] amongst others. These are generally referred to as porphyrinx–spacer–porphyrin (PSP) units or space-separated porphyrins.

In most of these studies, a fundamental aspect of the basic design has been to ensure that the size and shape of the molecular structure is well-defined. This is achieved using a multi-bridged polycyclic backbone, whose dimensions and geometry can be modelled with a high degree of confidence. The expectation,

[a]*Chemistry, School of Biological, Biomedical and Molecular Sciences, University of New England, Armidale, NSW, 2351, Australia. E-mail: mgunter@une.edu.au; Fax: +612 6773 3268; Tel: +612 6773 2767*
[b]*School of Chemistry, Physics and Earth Sciences, Flinders University, Bedford Park, Adelaide, SA, 5042, Australia. E-mail: Martin.Johnston@flinders.edu.au; Fax: +61 8 8201 290; Tel: +61 8 8201 2317*
[c]*Centre for Molecular Architecture, Central Queensland University, Rockhampton, Queensland, 4702, Australia*

reinforced by modelling studies, is that there is only limited flexibility within the backbone structure.

More recently, complexation studies of a series of rigid bidentate ligands spanning a range of sizes with selected metallated PSPs have indicated that there is a surprising lack of discrimination in the complexation effectiveness as measured by the various association constants.[10,13,16] These results suggest that there is considerable flexibility in these systems as regards porphyrin–porphyrin separation in the solution phase, and that this needs to be factored into any new designs so as to allow for a range of possible dimensions and geometries. Similar distortions from ideal calculated values have been observed in electrostatically driven geometry changes accompanying charge separation in supposedly rigid bichromophoric systems.[17]

To investigate these aspects more fully, we have undertaken a study of the solution-phase dimensions of a typical zinc-metallated PSP which is functionalised with a non-flexible probe within its U-shaped cavity (Fig. 1b). By careful selection of a series of both flexible and rigid bidentate ligands spanning a range of possible inter-ligand atomic distances we use thermodynamic and solution NMR measurements to gauge the dimensions and the flexibility of the host molecule.

Results and discussion

Synthesis

The syntheses of a variety of alkyl-substituted imides of the type **2** have been described previously.[7,14,18] These reactions make use of a simple two-step sequence involving heating of the appropriate aliphatic amine with the anhydride of diacid **1** over several days. Subsequent dehydration of the amic acid **3** by heating with sodium acetate in acetic anhydride gives the respective imide (Scheme 1).[19,20]

However, in our hands reaction of the anhydride with a variety of aromatic amines under mild to forcing conditions failed to produce significant yields of either the amic acids **3a**–**d** or the subsequent imides **4a**–**d**. The use of high-pressure (13 kBar, rt) conditions was moderately successful, although the major product was the *bis*-amide, rather than the amic acid. Furthermore, technical logistics of the high-pressure reactions limited the reactions to small scales, and the method was not generally applicable.

With relatively weakly nucleophilic substituted anilines, no amic acid was produced either by using temperatures ranging from ambient to 84 °C; by heating the reactants neat at higher temperatures; by addition of catalytic amounts of acid or base; or by the use of a dehydrating agent 1,3-dicyclohexylcarbodiimide (DCC) at room temperature or 62 °C. However, use of the known *exo*,*exo*-fused *bis*-oxabridged norbornene *bis*-acyl chloride derivative of **1**,[21] although moderately unstable, produced the amic acids in good yields with para-substituted anilines.

Treatment of amic acids **3a**–**d** with sodium acetate (NaOAc) in acetic anhydride (Ac_2O) at higher temperatures (120–130 °C) resulted in imide formation, although the yields were often low and unpredictable. In many instances unidentified by-products were observed presumably as a result of competing retro-Diels–Alder reactions to form furan and an oxa-bridged norbornene carboxylic acid. These retro-Diels–Alder reactions could be overcome to some extent by carrying out the reaction in a sealed tube in the presence of excess furan, although this again was experimentally inconvenient as well as introducing the possibility of alternative isomer production.

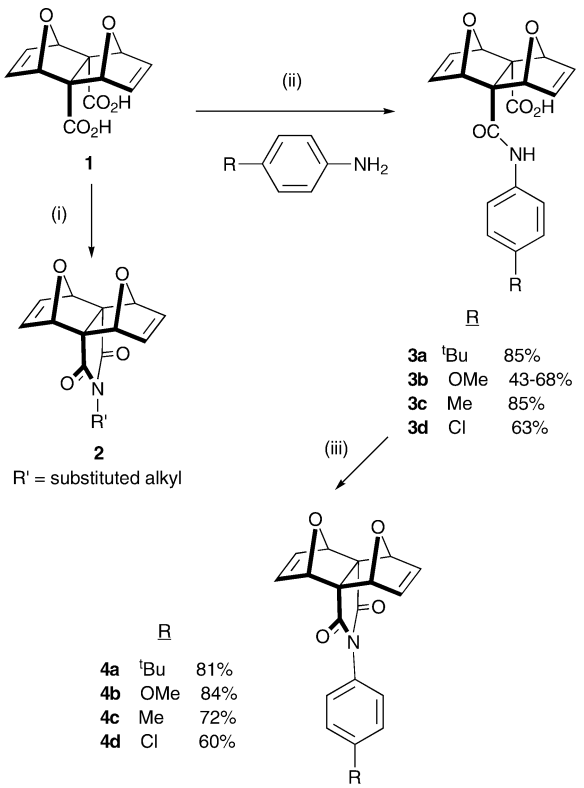

Scheme 1 Reagents and conditions: (i) $R'NH_2$, heat; NaOAc–HOAc, heat; (ii) PCl_5; (iii) EDC, HOBT, THF, rt.

Finally, the use of the reagent 1-(3-dimethylaminopropyl)-3-ethylcarbodiimide hydrochloride (EDC) in conjunction with 1-hydroxybenzotriazole (HOBT) under mild conditions (dry THF N_2 atmosphere, 3 d, rt) (Scheme 1) was found to produce the imides **4a**–**d** cleanly and in good yields.

Utilisation of the Mitsudo reaction,[22] catalysed by the ruthenium complex $RuH_2CO(PPh_3)_3$,[23] allowed the *bis*-cyclobutene diester adducts **5a** and **5b** to be prepared from consecutive cycloadditions of DMAD to the respective imides **4a** and **4b** (Scheme 2). The structural integrity and stereochemistry of the products were deduced from their ^{1}H NMR spectra where a new signal for the methine protons of the extended imides **5a** and **5b** (Scheme 2) at *ca.* 3.2 ppm replaces the alkenyl protons (*ca.* 6.7 ppm) of the starting compounds **4a** and **4b**, and a singlet at *ca.* 3.8 ppm appears for the methyl ester protons. The oxa-bridgehead protons in **5** resonate upfield in comparison to the starting compounds (*ca.* 4.8 ppm compared to *ca.* 5.3 ppm) due to the removal of the deshielding effects from the neighbouring double bond.

Two *bis*-epoxide derivatives **6a** and **6b** were prepared from **5a** and **5b** respectively in equally good yields (*ca.* 75%) using either ^{t}BuOOH and MeLi at −78 °C or ^{t}BuOOH and ^{t}BuOK at −5 °C in THF (Scheme 2). The ^{1}H NMR spectral pattern of the epoxides is very similar to that obtained from the cyclobutene esters **5**. However, characteristic changes in the chemical shifts of the oxa-bridge protons ($\Delta\delta$ *ca.* +0.75 ppm) and the cyclobutane protons ($\Delta\delta$ *ca.* −0.36 ppm) were as expected.[19,24]

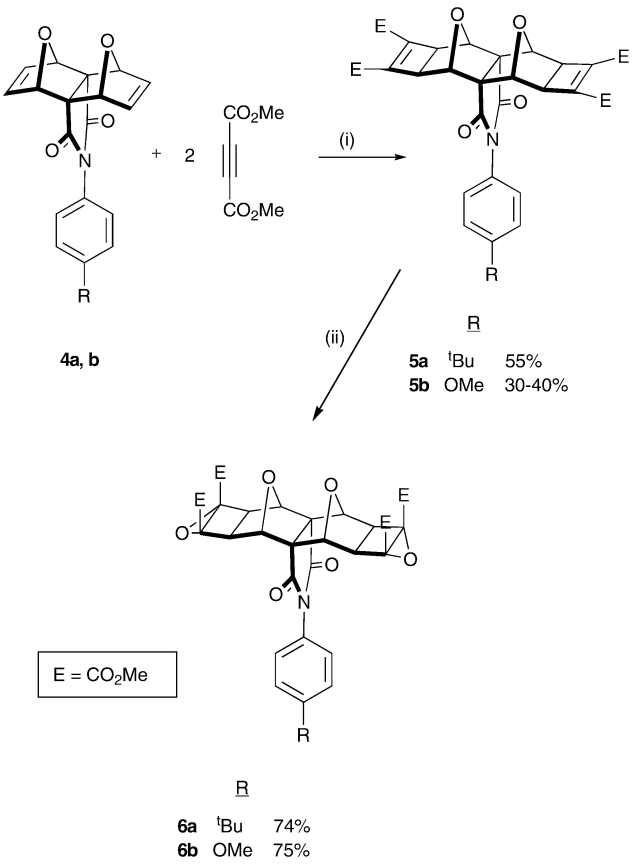

Scheme 2 Reagents and conditions: (i) $RuH_2CO(PPh_3)_3$; (ii) ^{t}BuOOH, MeLi, −78 °C or ^{t}BuOOH, ^{t}BuOK, −5 °C, dry THF, N_2.

For the production of U-shaped PSPs[14] the building block assembly approach utilising the ACE reaction (a 1,3-dipolar cycloaddition reaction between an alkene and a cyclobutane epoxide) was employed. In particular, **6** was linked with *tetrakis*-(3,5-di-*tert*-butylphenyl)porphyrin block **9** (^{t}BuPBlock). This block is based on porphyrin dione **7** and its extension with 1,2,4,5-benzenetetramine[25] subsequently developed by Warrener's group, has previously been synthesised by coupling **7** with a fused polycyclic norbornene dione **8** (Scheme 3).[26]

A number of *bis*-porphyrin systems, of different shapes and sizes, have been reported by using coupling reactions of **9** with various spacer groups, thus demonstrating the versatility of this building block.[8–10,15,26–28]

Thus ^{t}BuPBlock **9** and *bis*-epoxides **6** were heated in CH_2Cl_2 in a sealed tube at 150 °C for a period of 3 d, resulting in a 53% conversion into the desired PSP **10a** (Scheme 3) after purification and recrystallisation. The products were analysed by ^{1}H and ^{13}C NMR spectroscopy and all ^{1}H peaks were satisfactorily assigned with the aid of various 2D NMR techniques (COSY, 2D ROESY, CH correlation). The formation of a cavity type geometry is a direct result of the high *exo*,*exo*-stereoselectivity of these ACE reactions when a norbornene dipolarophile is employed.[26,28]

Bidentate ligand binding as a probe of cavity dimensions

We have previously reported a number of complexation studies on related open U-shaped PSP systems. In these instances we employed the complexation strengths of rigid *bis*-pyridine guests to obtain information regarding the cavity dimensions and flexibility of PSP hosts. The most extensively studied in this respect was a di-porphyrin host derived from the condensation of two equivalents of ^{t}BuPBlock **9** with an *s*-tetrazine coupling reagent.[9,10,28] Complex formation with a number of different sized *bis*-pyridine guests has been described, including a *bis*-norbornyl *s*-tetrazine adduct, a naphthyldiimide, a phenyldiimide, a *bis*-pyridine porphyrin, and a *tetrakis*-pyridine porphyrin.[8,10,11,13,16] The complexation of ligands in this series by the host molecule was estimated by molecular modelling to require contraction in the porphyrin centre-to-centre distance. In the case of smaller sized guests, large contractions of the cavity by approximately 7 Å is necessary, whereas a small contraction in the order of 2 Å was required for the ditopic binding of the larger guest molecules. Strong complexation in all cases suggests that these types of PSPs must be able to undergo significant geometric changes during complexation.[9]

In contrast to this, Sanders has described rigid cyclic porphyrin oligomers that exhibit extraordinary selectivity toward single *bis*- and *tris*-pyridine guests.[29,30] Due to the rigidity of the butadiyne linkage groups used and the additional control of the dimensions enforced by the cyclic structure of these systems, only the guest that closely complements the size and shape of the *bis*-porphyrin cavities was complexed strongly. Any larger guests that were not as complementary geometric matches to the cavity dimensions of the porphyrin macrocycles exhibited substantially weaker complexation. Nevertheless, subsequent studies on the selectivity and rate enhancement of Diels–Alder reactions inside these dimer and trimer cavities showed that some of these systems are remarkably flexible and they can distort for optimal stabilisation of the transition states.[31] This was not predicted by modelling studies, but even some of the crystal structures of these systems showed a surprising degree of distortion. Clearly, 'rigidity' is a term that should be used with caution even for those molecules where a simple structural diagram might predict restricted flexibility. Certainly for larger molecules even small changes in individual atomic parameters can quickly magnify into significant geometric distortions from a predicted inflexible structure.

Thus while not anticipating absolute rigidity, it was of interest to estimate the degree of flexibility that might be possible in the open U-shaped systems **10**, in comparison to inherently more constrained cyclic analogues. We now demonstrate how it is possible to use the concept of a 'molecular ruler' to compare the relative trends in ligand complexation strengths within a series of both flexible and rigid bidentate ligands to gauge the accessibility of the cavity to incoming ligands, and the range of dimensions possible in these apparently semi-rigid systems. For this purpose, we chose to use the U-shaped host **10b** as a representative, as its *t*-butyl group on the central aromatic ring provides a useful NMR probe that can be used in determining solution structures and conformations of any complex formed with *bis*-ligands.

Flexible ligands and the molecular ruler concept

The concept of a flexible 'molecular ruler' was introduced by Crossley to determine the stereochemistry of a series of linked porphyrins.[32] The main concepts, as applied to our systems, are delineated here. Assuming that the cavity of the PSP is a well-defined rigid structure, a flexible ditopic ligand that is too short to span the porphyrin-to-porphyrin distance will not exhibit a

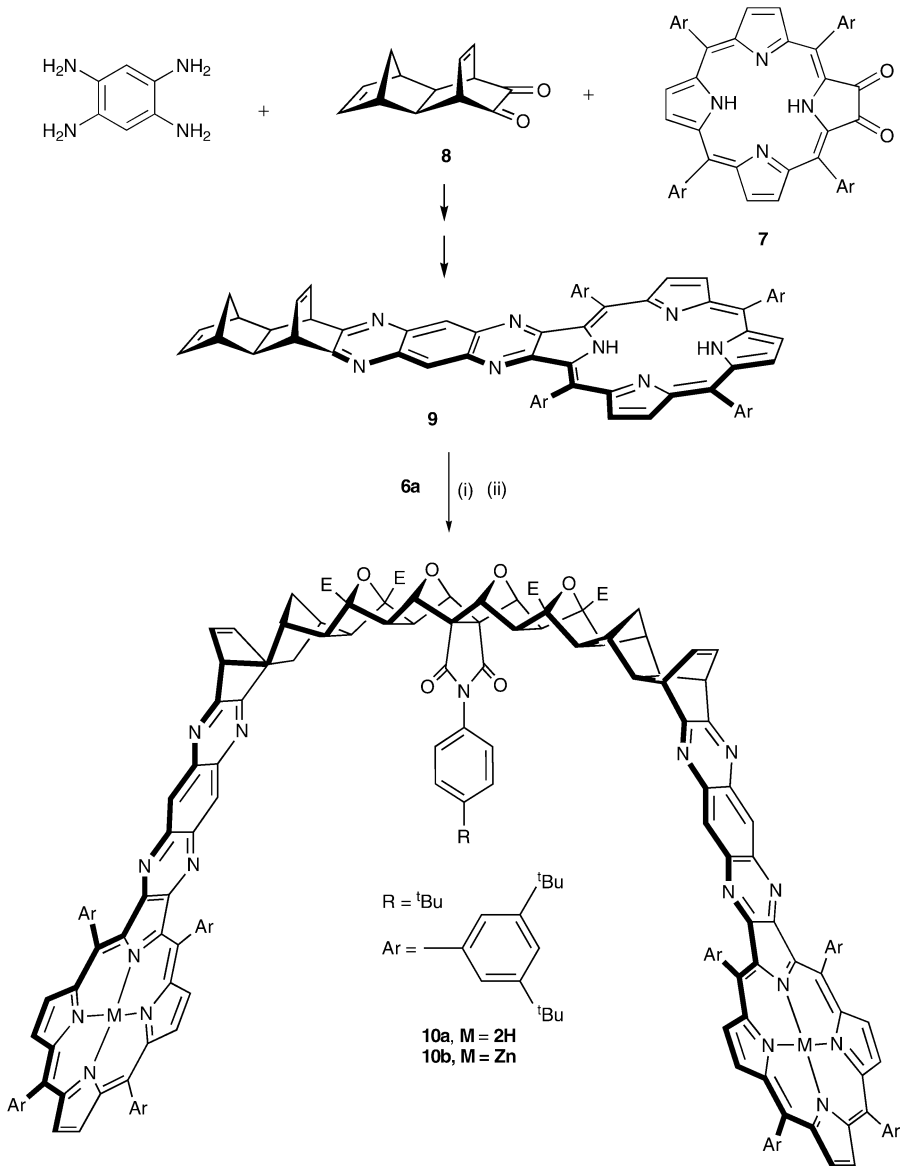

Scheme 3 Reagents and conditions: (i) CH_2Cl_2, sealed tube, 190 °C, 90 h. (ii) $Zn(OAc)_2$, $CHCl_3$–MeOH.

significant chelate effect due to the induced strain (an enthalpic energy cost) that would accompany the doubly complexed state. If on the other hand the ditopic ligand is much longer than the porphyrin-to-porphyrin distance then a considerable loss of rotational freedom (an entropic energy cost) is expected upon complex formation. A flexible ditopic ligand of complementary length, therefore, should have a measurably enhanced chelate effect associated with complex formation. In other words the concept uses the maximum calculated N–N distance of each flexible ligand to probe the porphyrin-to-porphyrin (and hence cavity) dimensions using each guest as a molecular tape measure of fixed maximum length.

For a series of flexible ligands covering a range of lengths, a number of hydroxyether derivatives of naphthalene-1,5-diol were esterified with nicotinic acid to form a series of *bis*-pyridine guests **11a**–**e**. The geometries of all structures were calculated using a molecular mechanics force field (MMFF94) as well as a semi-empirical method (AM1). The calculated N–N distances for the fully extended conformers of these guests ranged from 15.4 Å for **11a** to 31.9 Å for **11e**. The N–N and estimated Zn–Zn distances calculated using the three protocols for each of the *bis*-pyridine guests are presented in Table 1. The best fit between host and guest was expected for **11b** since it has an estimated N–N distance of 22.7 Å (AM1), which is very close to the calculated ideal porphyrin-to-porphyrin distance of 22.9 Å calculated for **10b**†. This was indeed the case with a 100 fold larger association constant observed for **11b** over any other guest examined (Table 1). This provides confidence in the methodology, with a good match between calculated host and guest dimensions correlating with a maximum in the association constant.

† Calculated from the Zn–Zn distance of 27.3 Å for **10** (AM1) with added empirical Zn–N bond distances of 2.2 Å.

Table 1 Calculated N–N and Zn–Zn interatomic distances, and association constants determined for the complexation of pyridine and the series of flexible *bis*-pyridine guests **11a**–**e** with a monomeric porphyrin host **9** and a *bis*-porphyrin host **10b** in CH_2Cl_2 at 25 °C

	Calculated N–N distance/Å			Binding constants/L mol^{-1}	
Guest	MMFF94	AM1	Calculated 'ideal' Zn–Zn distance/Å[a]	Zn^{t}BuPBlock **9**	Zn_2PSP **10b**
Pyridine	—	—	—	1.26×10^4	9.8×10^3
11a	15.0	15.4	19.8	9.1×10^3	1.09×10^5
11b	22.8	22.7	27.1	5.8×10^3	1.34×10^6
11c	25.0	25.0	29.4	5.2×10^3	9.5×10^4
11d	27.7	27.7	32.1	1.00×10^4	8.0×10^5
11e	32.7	32.6	37.0	2.2×10^3	9.8×10^3

[a] Calculated from the N–N distance (AM1) + 4.4 Å, for two Zn–N bonds.

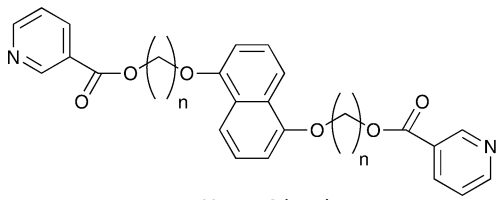

The methods used for analysing the complexes formed between ditopic hosts such as the *bis*-zinc derivative of PSP **10b** and various bidentate ligands such as these *bis*-pyridine guests have been widely used and the theory is well established. The calculation of association constants from UV-Vis spectral analysis was based on the assumption of the formation of a 1 : 1 complex in all cases; this was supported by the presence of well-defined isosbestic points.

A more rigorous method, used extensively by Sanders, to determine chain length selectivity relies on the calculation of the 'effective molarity' (EM) or chelation factor rather than a direct comparison of association constants. The effective molarity is best understood as the nominal concentration of a catalytic group that would be required in an intermolecular process to match the rate of the equivalent intramolecular reaction. It has the dimensions of molarity, and can thus be considered as a 'chelation factor' which can give an indication of the complexing effectiveness of a bidentate ligand in a ditopic host. A schematic view of the binding of a bidenate ligand (LL) to a metallated *bis*-porphyrin (MM) is shown in Fig. 2. Assuming independent complexation events at each end of the ditopic host–bidentate guest system (*i.e.* non-cooperative complexation), the EM for the second complexation of a bidentate ligand (guest) can be defined using eqn (1):

$$\mathrm{EM} = \frac{K_{\mathrm{LLMM}}}{K_1^2} \quad (1)$$

where: K_1 = the microscopic binding constant for each M–L interaction and is estimated by eqn (2),

$$K_1 = \frac{K_{\mathrm{LLM}}}{K_{\mathrm{LM}}} \times \frac{K_{\mathrm{LLM}}}{2} \quad (2)$$

and where K_{LLMM} = the macroscopic binding constant for complexation between bidentate ligand (LL) and *bis*-porphyrin host (MM); K_{LMM} = the macroscopic binding constant for complexation between monodentate ligand (L; pyridine) and *bis*-porphyrin (MM); K_{LM} = the macroscopic binding constant for complexation between monodentate ligand (L) and a mono-porphyrin analogue (M); and K_{LLM} = the macroscopic binding constant for complexation between bidentate ligand (LL) and mono-porphyrin analogue (M).

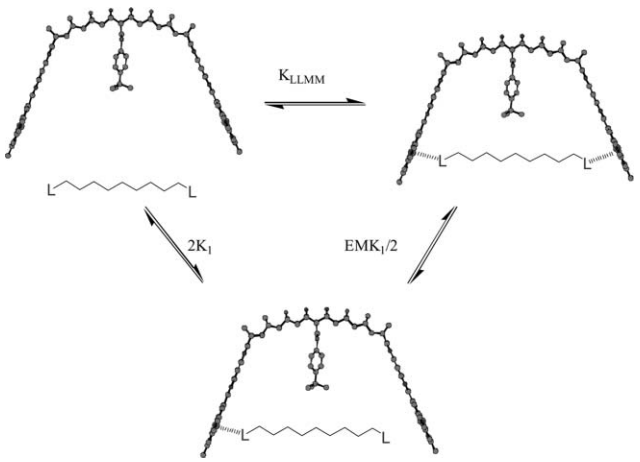

Fig. 2 Binding cycle of a PSP (MM) with a bidentate ligand (LL) and the relationship between macroscopic (K_{LLMM}) and microscopic (K_1) binding constants and effective molarity (EM).

In this way, the EMs for each of the flexible *bis*-pyridine series of ligands **11a**–**e** complexing to **10b** can be calculated, and a comparison made between these and the calculated N–N distances. The results are shown in Fig. 3.

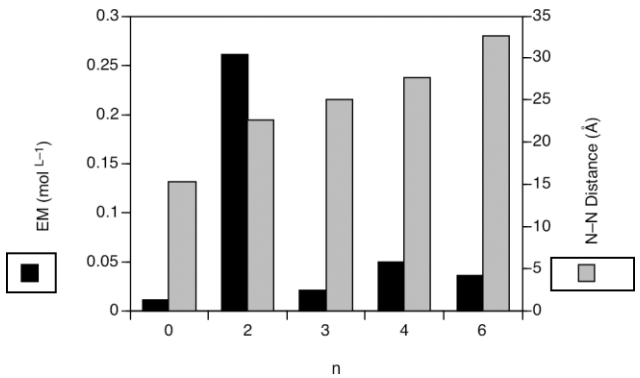

Fig. 3 Calculated effective molarities (EMs) and calculated N–N distances for each member of the flexible *bis*-pyridine series of ligands: $n = 0$ (ester **11a**), $n = 2$ (**11b**), $n = 3$ (**11c**), $n = 4$ (**11d**) and $n = 6$ (**11e**)] showing a maximum for **11b** ($n = 2$) which has an N–N distance of 22.7 Å (AM1).

Accessibility of the cavity

Within the Sanders method for calculating effective molarities is the factor K_{LMM}/K_{LM} which is often referred to as the 'accessibility factor' for a cavity or cyclic structure. In this way the ability of a guest to access the inner cavity of a host may be quantified. Values of 1 indicate an open accessible cavity with no steric impediments to complexation, whereas a value of zero indicates an essentially closed host.

The assumption used in determining the accessibility factor, K_{LMM}/K_{LM}, is that one porphyrin unit in Zn_2PSP **10b** complexes any pyridine ligand more or less as strongly as the corresponding monomeric analogue, Zn^{t}BuPBlock **9**, by a common factor. This assumption simplifies the process considerably as a single ratio of K_{LMM}/K_{LM} using pyridine as the ligand (L) can be used for all EM determinations. Association constants for monodentate ligand pyridine (L) with both Zn^{t}BuPBlock **9** (M) and Zn_2PSP **10b** (MM) (Fig. 2 and Table 1) were each calculated from non-linear least squares curve fitting of absorption changes at 426 nm (host maximum) and 434 nm (complex maximum). The presence of isosbestic points at around 430 nm for both host–pyridine titrations indicated the presence of just two absorbing species (host and complex) in each case supporting the assumption of 1 : 1 complex formation and 1 : 2 complex formation,‡ respectively. The ratio K_{LMM}/K_{LM} was thus calculated to be 0.8 (0.98/1.26). A value of 0.8 for the accessibility factor indicates that the cavity of Zn_2PSP **10b** is reasonably open and accessible but there may be a small steric impediment to complexation compared with Zn^{t}BuPBlock **9**. This is presumably caused by the presence of the bridging scaffold which limits accessibility of an approaching ligand in **10b** compared to **9**.

The accessibility factor ($K_{LMM}/K_{LM} = 0.8$) was used in subsequent calculations of effective molarities (EMs) according to eqn (1) and (2).

A comparison of the binding constants measured by UV-Vis spectroscopic methods for the various flexible *bis*-pyridine guests with Zn^{t}BuPBlock **9** is shown graphically in Fig. 4. Differences in binding strengths to the monozinc porphyrin analogue were evident which underscores the importance of determining EMs rather than directly comparing association constants. All K_{LLM} values measured were within an order of magnitude of each other with no obvious relationship between guest structure and binding strength.

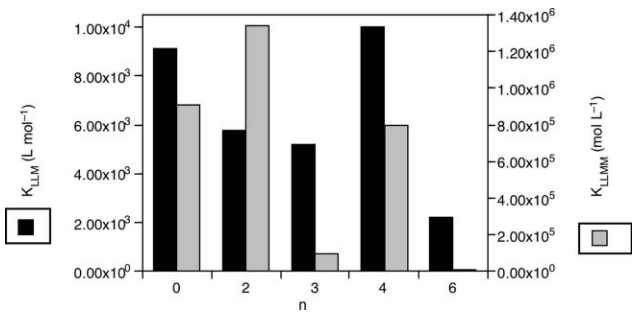

Fig. 4 Binding constants (K_{LLM}) for binding of each member of the flexible *bis*-pyridine series of ligands $n = 0$ (ester **11a**), $n = 2$ (**11b**), $n = 3$ (**11c**), $n = 4$ (**11d**) and $n = 6$ (**11e**)] with Zn^{t}BuPBlock **9** (dark columns) and Zn_2PSP **10b** (shaded columns) in CH_2Cl_2 at 25 °C.

‡ It is assumed that the complexation of pyridine with each porphyrin unit of the *bis*-porphyrin host is non-cooperative.

A comparison of binding constants for the flexible guests **11a**–**e** and Zn_2PSP **10b** revealed that two guests, **11b** and **11d**, were more strongly bound to the *bis*-porphyrin host compared to the other flexible *bis*-pyridine guests (Fig. 4). The selectivity of Zn_2PSP **10b** toward **11b** was further emphasised by the more reliable comparison of calculated chelating factors (Fig. 3). These results indicate that Zn_2PSP **10b** has a well-defined cavity with the distance between the zinc metal centres being in the region of 22.7 Å, which is in excellent agreement with the ideal N–N distance predicted by molecular modelling (22.9 Å). It should be noted that all EM values were relatively small in absolute terms compared to the maximum of around 100–400 M predicted for a strain-free chelate between a porphyrin dimer host and a perfectly complementary dipyridine guest as estimated by Sanders *et al.*[29] and this reflects the known conformational mobility of the guests **11a**–**e** and may also indicate some degree of freedom in the *bis*-porphyrin **10b** host system.

Rigid ligands—flexibility of the host

In addition to the flexible *bis*-pyridine ligands so far discussed a series of rigid *bis*-pyridine guests **12**–**14** were also synthesised using published procedures. The optimised geometries of these rigid *bis*-pyridine guests were calculated using semi-empirical molecular models (AM1), and the N–N distances are indicated on the structures.

For the rigid *bis*-pyridine guests, limited solubility of the perylene diimide **12** precluded measurements of an association constant, but values for the other porphyrin-based guests could be obtained by UV-Vis titrations in a similar manner to that outlined above. Significant absorbance corrections were required for strongly absorbing guests. The measured binding constants for **13** and **14** binding with Zn_2PSP **10b** were 2.6×10^7 M^{-1} and 1.5×10^7 M^{-1} in CH_2Cl_2 at 25 °C, respectively.

The similar binding constant values of these two porphyrin guests of different size is remarkable, and suggests that the *bis*-porphyrin **10b** is able to undergo relatively large conformational changes with a relatively small energy cost. In order to further investigate the conformational mobility and complexation geometry of **10b** upon binding with the smaller *bis*-pyridine porphyrin guest **14**, a number of NMR binding experiments were conducted.

NMR studies of complex conformation

In the ^{1}H NMR spectrum of an equimolar solution of Zn_2PSP **10b** and **14** in $CDCl_3$ at 30 °C the chemical shifts of the resonances assigned to the bound porphyrin guest **14** were significantly different from those of the unbound guest (Table 2 and Fig. 5). Some degree of broadening of the resonances for **14** was evident in the spectrum.

The large upfield shifts of the α-pyridyl (−5.7 ppm) and β-pyridyl (−1.7 ppm) proton resonances measured are typical of pyridine binding axially to a zinc porphyrin.[33] The upfield shifts of the β-pyrrole (−1.3 ppm) and inner NH (−0.9 ppm) proton resonances of **14** were also consistent with simultaneous

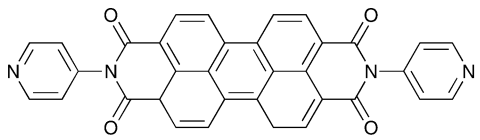

12

N - N distance = 20.0 Å

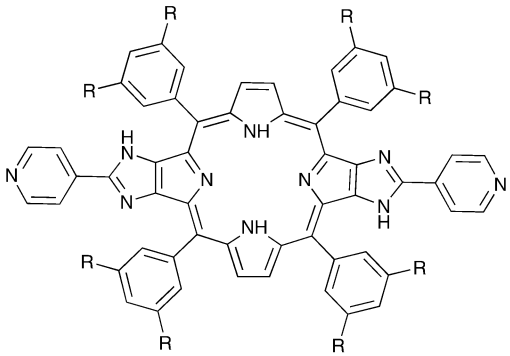

13

N - N distance = 21.4 Å

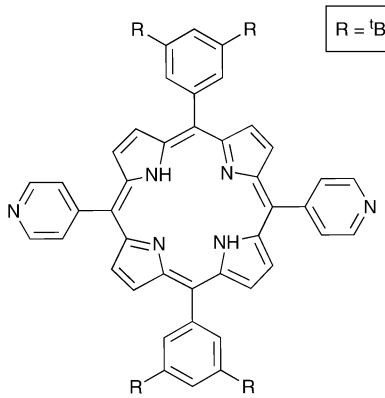

14

N - N distance = 15.6 Å

complexation with both porphyrin units within **10b**. At 20 °C the peaks of **14** were all sharpened compared to the spectrum obtained at 30 °C with no changes in chemical shifts. No significant changes in the resolution of these peaks or the host **10b** peaks occurred at lower temperatures (−50 °C). Together with the large binding constant measured by UV-Vis methods (*ca.* 1.5×10^7 L mol^{-1}), this result supports the premise that the spectra obtained near room temperature are of a 1 : 1 complex in slow exchange on the NMR timescale in the absence of unbound guest.

Complete free rotation of guest **14** within the cavity of host Zn_2PSP **10b** is precluded because of the large size of **14** [width approx. 20 Å]. The simple NMR spectral pattern of the bound guest **14**, along with the chemical shift changes, suggests that on average a symmetrical 'horizontal' (or flat) binding geometry of the guest porphyrin ring system within the cavity of Zn_2PSP **10b** is maintained. A single peak for each of the α-pyridyl protons over a range of temperatures (−50 to 30 °C) indicates a symmetrical binding geometry in **10b** with a parallel cofacial arrangement of the two porphyrin rings of **10b** with orthogonally bound pyridine groups. Indeed molecular modelling calculations (AM1)

Table 2 Chemical shift changes of the guest **14** (G) and host **10b** (H) in an equimolar mixture of the each ($CDCl_3$, 30 °C). All assignments were supported by results from 2D NMR spectral analyses

Peak assignment	Unbound shift (ppm)	Bound shift (ppm)	$\Delta\delta$
α-Py	9.03	3.36	−5.67
β-Py	8.18	6.48	−1.70
βG	8.95	7.55	*ca.* − 1.3
β′G	8.81		
bG	8.08	8.17	+0.09
dG	7.83	7.70	−0.13
'Inner' NH	−2.76	−3.63	−0.87
^{t}BuG	1.53	1.36(*broad*)	−0.17
^{t}Bu c 'probe'	0.94	−0.17	−1.11
β,β′(H)	8.94	8.97	+0.03
β″(H)	8.83	8.85	+0.02
q	8.55	8.50	−0.05
d′	8.05	8.17*and*8.07	+0.12*and* + 0.02
d	7.94	8.00*and*7.94	+0.06*and*0.00
e	7.91	7.87	−0.04
e′	7.77	7.76	−0.01
b	7.26	6.73	−0.53
a	6.92	6.73	−0.19
7	6.53	6.49	−0.04
6	4.69	4.63	−0.06
1	4.24	4.16	−0.08
E	3.93	3.87	−0.06
5	2.43	2.35	−0.12
3	2.37	2.31	−0.06
H_a	2.16	2.17	+0.01
H_b	2.03	2.04	+0.01
2	1.91	1.75	−0.19
4	1.87	1.72	−0.12
^{t}Bu′	1.52*and*1.50	1.51*and*1.49	−0.01*and* − 0.01
^{t}Bu	1.46*and*1.45	1.44*and*1.39	−0.02*and* − 0.06

[a] (G = guest, H = host).

indicate that with a defined Zn–Zn distance of 20.0 Å required to accommodate guest porphyrin **14**, the porphyrin rings of **10b** are essentially parallel (Fig. 5)§.

The most significant change in the NMR spectrum of Zn_2PSP **10b** (Table 2) upon mixing with **14** was the large upfield shift (−1.1 ppm) of the resonance assigned to the ^{t}Bu(imide) group of the central aromatic ring. This 'probe' signal confirms the binding of the *bis*-pyridine guest within the cavity of the host **10b**. (Molecular modelling indicates a distance of 3.6–4.0 Å between a hydrogen of the pendant tertiary butyl group and the mean plane of the four nitrogen atoms in the centre of porphyrin **14** bound within the cavity).

The magnitude of the changes in chemical shift of the b (−0.53 ppm) and a (−0.19 ppm) resonances of Zn_2PSP **10b** were also consistent with the protons being positioned above the porphyrin ring of the guest **14**. Smaller changes in chemical shift for resonances of protons along the backbone of the *bis*-porphyrin system **10b** were also consistent, considering the relative distance of each proton from a porphyrinic guest bound horizontally across the cavity of Zn_2PSP **10b**. More specifically the 'downward' facing protons (2, 4 and 5) were all shielded (−0.19, −0.12 and

§ It has been shown in other related *bis*-porphyrin structures with semi-rigid bridges that a non-parallel orientation of the lateral porphyrin units results in inequivalence of the Zn-bound pyridine α-proton resonances of a bound dipyridyl porphyrin similar to that described here.[10]

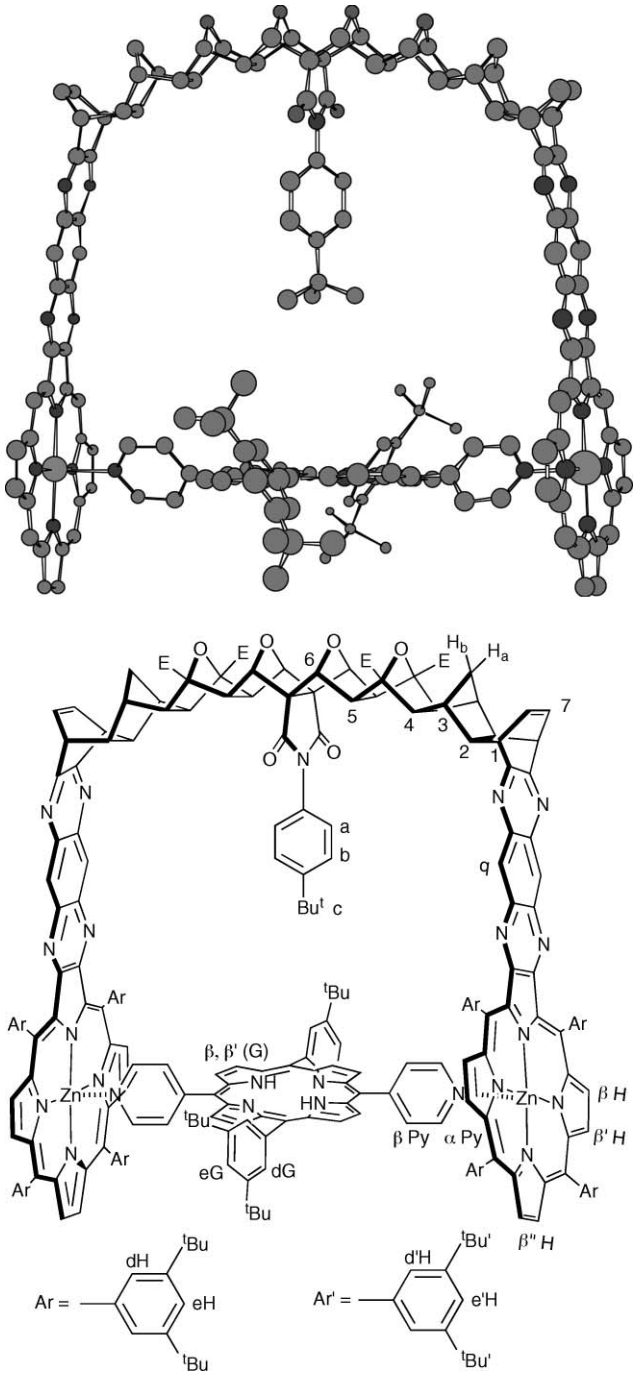

Fig. 5 Conformation (top) of the 1 : 1 complex of **10b**–**14** deduced from molecular modelling (MM2 and AM1) and NMR studies indicating the essentially parallel orientation of the porphyrin subunits. The hydrogens, ester and *meso*-aryl groups have been omitted for clarity. The Zn–Zn distance is 20.0 Å. The lettering and numbers in the bottom Fig. refer to the proton resonance assignments described in Table 2.

−0.12 ppm, respectively) slightly more than the 'upward' facing protons (1, 3 and 6; −0.08, −0.06 and −0.06 ppm, respectively). Overall the resulting NMR spectrum can be rationalised by a strongly bound (slow exchange, bound signals only) porphyrin guest **14** that has a symmetrical horizontal binding geometry of the porphyrin ring (Fig. 5).

A parallel NMR study of the binding of the larger porphyrinic guest **13** with **10b** was not as informative. In this case the resonances of the guest itself are broadened at ambient temperature, and appear as overlapping sets of peaks at lower temperatures as a result of tautomerism involving the inner N–H and imidazole NH protons, as noted previously for related systems.[34] Similar problems were encountered in the NMR spectra of a 1 : 1 mixture of **13** and **10b**, with broadened and multiple sets of resonances. Nevertheless, the α and β-protons of the pyridyl moieties of the bound guest **13** were identified at 2.88 and 5.77 ppm, respectively, and the *t*-Bu probe signal was at 0.04 ppm. The similarities of these shifts and others that could be assigned to those of the **10b**–**14** complex are evidence of a similar binding geometry to that of the smaller porphyrinic guest **14**.

For the association of perylene diimide **12** with **10b** an NMR study also provided evidence for a 1 : 1 complex with the diimide bridging the two metalloporphyrin units, similar to the conformation of **10b**–**14**. The diimide **12** itself is essentially insoluble in $CDCl_3$; however, stirring and sonication of an excess of **12** with a solution of **10b** in this solvent over several hours resulted in its gradual solubilisation. The excess solid was filtered off, and the NMR spectrum of the resulting solution indicated that a 1 : 1 complex had formed. Although some of the resonances were broadened at room temperature, the spectrum at 0 °C was well resolved and showed characteristic metal-bound pyridine β and α pyridine protons at 5.62 and 3.10 ppm together with an apparent AB quartet for the perylene aromatic protons at 8.19 ppm. Although direct correlation of absolute chemical shift changes is precluded by the insolubility of **12** in $CDCl_3$, the shifts in the complex can be compared to those of the diimide **12** in trifluoroacetic acid; the $\Delta\delta$ values for the α- and β-pyridyl and the aromatic protons are then −5.83, −2.73 and −0.7 ppm, respectively. Crucially, the t-butyl probe signal was shifted by −0.23 ppm relative to its position in **10b**, clearly indicating shielding by the coordinated perylene diimide in a horizontal conformation (indeed modelling studies indicated that a 'perpendicular' conformation would be precluded by close contacts within the van der Waals radii of the pendant t-butyl group).

The results of this study of 1 : 1 complex formation between Zn_2PSP **10b** and various sized rigid guests infers that a significant variation of the overall molecular dimensions of the host system is possible. A method that can be applied to the investigation of molecular size is an NMR technique based on diffusion processes in solution, namely diffusion ordered spectroscopy (DOSY) and we were encouraged to apply it to these systems.

Diffusion (DOSY) NMR—estimating the overall dimensions

The DOSY NMR method has been applied by other workers to the study of molecular complexes that are bound by non-covalent forces[35] including a study of a dimeric molecular capsule that demonstrated a strong correlation between average calculated molecular radii (AM1) and experimentally determined spherical radii (r_s).[36] In the current study 2D DOSY NMR has been used to investigate overall or gross molecular size changes due to complex formation between the Zn_2PSP host **10b** and **14**.

A 2D DOSY NMR spectrum was acquired from the solution of a 1 : 1 mixture of Zn_2PSP **10b** and **14** in $CDCl_3$ at 30 °C. If slow

exchange conditions are assumed the single band observed at a single diffusion constant (D) of 5.7 ($\pm$0.5) $\times$ 10^{-10} m^2s^{-1} indicates the presence of a single species (1 : 1 complex) in solution (Fig. 5). The equivalent spherical molecular radius (r_s) was calculated to be 7.5 ($\pm$0.7) Å.

For comparative purposes a small library of molecular spherical radii was generated through a series of 2D DOSY NMR experiments performed under similar conditions of solvent ($CDCl_3$) and temperature (30 °C). A graphical representation of all molecules and their respective molecular spherical radii (r_s) is presented in Fig. 6.

¶ Errors were estimated from the width of the 2D DOSY spectral band which is correlated with the curve-fitting error.[37]

An obvious trend exists between the size of the molecules, as determined by molecular modelling, and the respective spherical radii (r_s) determined experimentally using DOSY NMR. However, several important considerations must be made when interpreting the experimental results; (i) the hard-sphere approximation used in the Stokes–Einstein equation used for the calculation of D is not a realistic representation of the various shapes of all the molecules being studied and (ii) the rate of diffusion in solution is not solely dependent on molecular size but also on the strength of solute–solvent interactions. Solute–solvent interactions will vary depending on the type of functional group(s) attached to the solute (and solvent) molecules. It is possible that two molecules of similar size and shape, but with different functionality, may diffuse at significantly different rates in the same solvent. However, as very

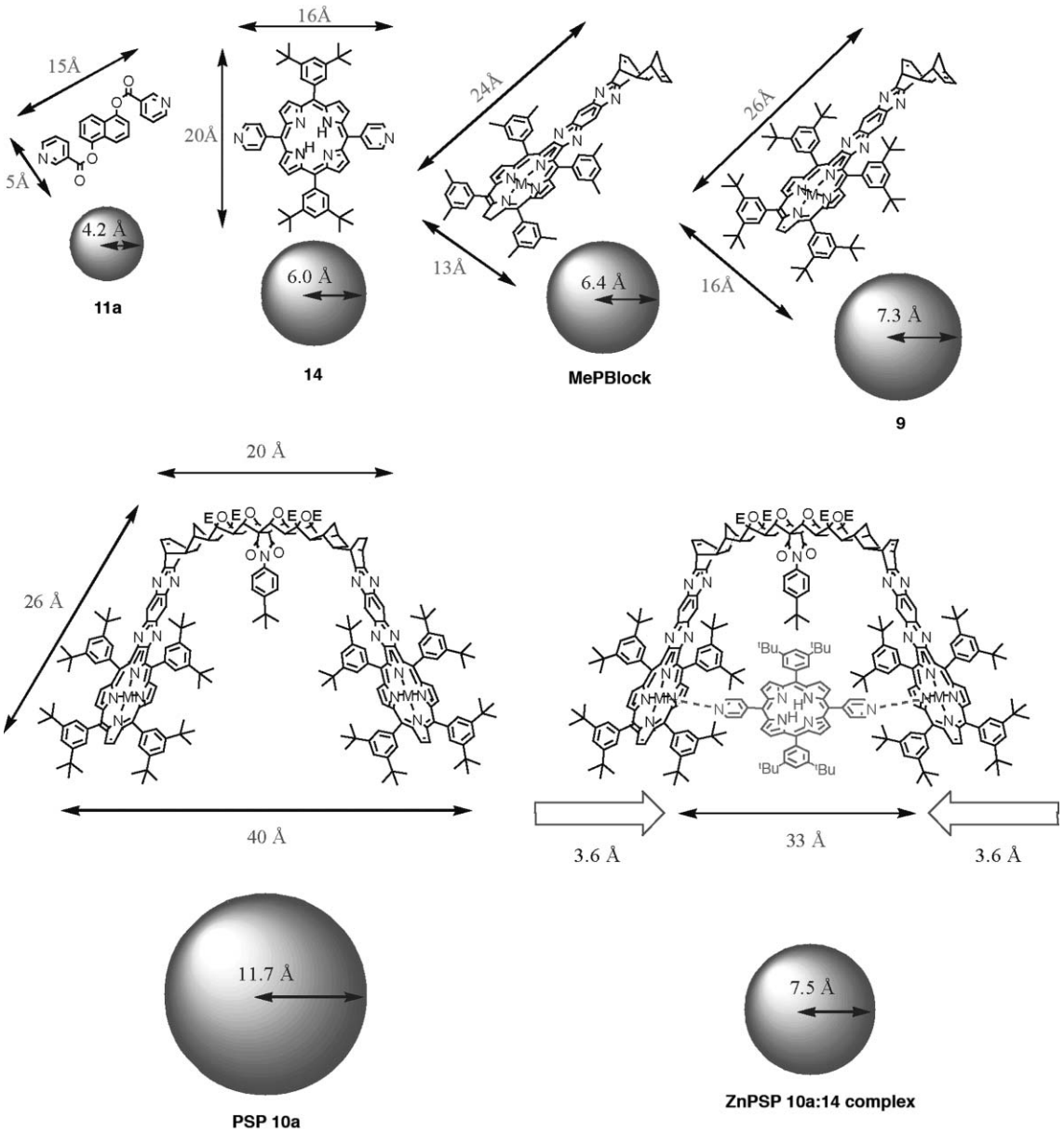

Fig. 6 A comparison of experimentally determined spherical radii (r_s) of a number of molecules including the Zn_2PSP **10b** and a 1 : 1 complex formed between **10b** and **14**. Errors range from 7% (r_s of **11a**) to 14% (r_s of **14** and **10b**).¶ Approximate molecular dimensions from computational modelling calculations (AM1) are shown on the structures, and radii calculated from the DOSY NMR experimental data are indicated on the spheres.

similar types of molecules are being compared in this study [*e.g.* Zn_2PSP **10b** and a 1 : 1 complex of **10b** and **14**], large changes in the diffusion rate have been interpreted as being due to changes in molecular (or aggregate) shape and size.*

It is clear from the comparisons made in Fig. 6 that a considerable contraction, indicated by a decrease in the spherical radius (r_s), must occur upon complex formation between Zn_2PSP **10b** and **14** compared with the free host **10b**. This is consistent with a closing of the two porphyrin 'jaws' of the host system onto the *bis*-pyridine porphyrin guest **14** as it ditopically binds within the cavity of **10b**.

Conclusions

We have successfully extended the building block approach toward *bis*-porphyrin cavities to synthesise an open framed U-shaped cavity containing an internally oriented pendulous group.

This success should allow greater diversity in the design of these types of molecules that might be adapted for specific purposes, particularly those involving switching processes mediated by photochemically induced electron or energy transfer.

Nevertheless, from the studies presented here for a series of ligands over a range of dimensions, it is clear that care needs to be exercised in the design of apparently 'rigid' open-framed systems, especially those which contain large or extended backbones, as small degrees of flexibility within each modular section can be amplified across the molecule as a whole. For smaller molecules, a price for more rigidity might well be at the expense of the accessibility of the cavity for intended internal ligands. Each of these factors should be included in any future design of purpose-built systems.

Experimental

General

All solvents were distilled before use by using standard procedures. Tetrahydrofuran (THF) was distilled over sodium using benzophenone as an indicator of water content; pyridine was stored over KOH and molecular sieves (type 3 Å) for a minimum of 6 h and then distilled over $LiAlH_4$. and stored over KOH/molecular sieves (type 3 Å); triethylamine (Et_3N) was distilled over CaH_2; benzene was dried over sodium wire; AR grade acetonitrile (MeCN) and dimethylformamide (DMF) were both dried over type 3 Å molecular sieves. Flash column chromatography was carried out using either aluminium oxide, activated, neutral (Brockmann I standard grade) or silica gel (grade 9385, 230–400 mesh). Preparative TLC was performed on 20 × 20 cm glass plates coated with 0.5 mm thick Art. 7731 Kieselgel 60 G Merck silica.

NMR spectra were acquired using a 300 MHz Bruker AC-300P FT spectrometer. Chemical shifts (δ) are reported in parts per million (ppm) relative to the residual solvent. Coupling constants are reported in hertz (Hz). Gradient COSY, one-bond C–H correlation (HMQC), long-range C–H correlation (HMBC), 2D gradient NOESY, 2D ROESY and 2D DOSY experiments utilised standard BRUKER pulse programs and standard BRUKER parameters. UV-Vis spectra were recorded on a Varian Cary IE UV-VIS spectrophotometer. IR spectra were recorded on a either a Perkin-Elmer FT-IR 1600 series or a Perkin-Elmer FT-IR 1725X series spectrophotometer. Melting points were determined using a Reichert microscopic hot-stage apparatus. High-pressure reactions and high-resolution EI and ES mass spectrometric analyses were carried out at the Centre for Molecular Architecture, Central Queensland University, Rockhampton, Queensland.

Molecular modelling was carried out using the Spartan software package [v4.0 (MM2) or 5.0 (MMFF94 and AM1, Wavefunction Inc.] on a Silicon Graphics O_2 workstation.

Synthetic procedures

Amic acids general procedure A. A solution of the *bis*-acyl chloride of **1**[21] (442 mg, 1.54 mmol), the appropriate substituted aniline (1.56 mmol) and pyridine (250 mg, 3.16 mmol) in $CHCl_3$ (15 mL) was stirred under N_2 for 5 d at room temperature in darkness. The reaction mixture was poured into water (20 mL) and the organic layer separated. The aqueous layer was extracted with $CHCl_3$ (4 × 5 mL) and the combined organic layers washed with water (5 × 20 mL). The organic layers were dried over Na_2SO_4 (anhydrous) and the solvent removed under reduced pressure to give the crude product. In some instances further purification was carried out, but generally the crude products were used directly in the subsequent preparations without further characterisation other than satisfactory ^{1}H NMR spectra.

1α,2β,3α,6α,7β,8α-*N*-(4-tert-butylphenyl)-11,12-dioxatetracyclo-[6.2.1.1^{3,6}.0^{2,7}]dodeca-4,9-dien-2,7-dicarboxamic acid (3a). The residue from general procedure A was dried under vacuum overnight giving the crude amic acid as a brown solid (85%) which was recrystallised from EtOAc–hexane and further purified by flash column chromatography [silica, EtOAc–hexane (1 : 1)] to give a white solid, mp 200–201 °C; ^{1}H NMR ($CDCl_3$) δ 7.31 (2H, m, Ar), 6.96 (2H, m, Ar), 6.81(2H, m) 6.73 (2H, m), 5.39 (2H, bs), 5.26 (2H, bs), 1.29 (9H, s).

1α,2β,3α,6α,7β,8α-*N*-(4-methoxyphenyl)-11,12-dioxatetracyclo-[6.2.1.1^{3,6}.0^{2,7}]dodeca-4,9-dien-2,7-dicarboxamic acid (3b). The product was purified by recrystallisation from $CHCl_3$–MeOH giving white needles (43%); mp 214–215 °C; ^{1}H NMR ($CDCl_3$) δ 7.05 (2H, m, Ar) and 6.82 (2H, m, Ar), 6.80 (2H, m), 6.73 (2H, m), 5.38 (2H, bs), 5.26 (2H, bs), 3.78 (3H, s).

1α,2β,3α,6α,7β,8α-*N*-(4-methylphenyl)-11,12-dioxatetracyclo-[6.2.1.1^{3,6}.0^{2,7}]dodeca-4,9-dien-2,7-dicarboxamic acid (3c). The remaining residue was dried under vacuum overnight giving the crude amic acid as a cream-coloured solid (85%); the product was further purified by recrystallisation from $CHCl_3$ giving a fine white powder after drying; mp 209–212 °C; ^{1}H NMR ($CDCl_3$) δ 7.38 (2H, m, Ar), 7.08 (2H, m, Ar), 6.75 (2H, m), 6.56 (2H, m), 5.32 (2H, bs), 5.15 (2H, bs), 2.29 (3H, s).

1α,2β,3α,6α,7β,8α-*N*-(4-chlorophenyl)-11,12-dioxatetracyclo-[6.2.1.1^{3,6}.0^{2,7}]dodeca-4,9-dien-2,7-dicarboxamic acid (3d). The remaining residue was dried under vacuum overnight giving the crude amic acid as a light brown solid. The product was purified by

* For a more reliable quantitative interpretation a much larger and more diverse library of molecules, along with a more complex mathematical analysis of molecular shape, would be needed but this was beyond the scope of the present study. These experiments were designed to seek further evidence for a contraction of the host **10** cavity upon formation of a 1 : 1 complex with **14**.

flash column chromatography (silica, $CHCl_3$) and dried overnight under vacuum giving a cream-coloured powder (63%); mp 210–214 °C; ^{1}H NMR ($CDCl_3$) δ 7.46 (2H, m, Ar), 7.24 (2H, m, Ar), 6.73 (2H, m), 6.57 (2H, m), 5.31 (2H, bs), 5.16 (2H, bs).

1α,2β,3α,6α,7β,8α-*N*-(4-tert-butylphenyl)-11,12-dioxatetracyclo-[6.2.1.1^{3,6}.0^{2,7}]dodeca-4,9-dien-2,7-dicarboximide (4a).

Method 1. The amic acid **3a** (1.05 g, 2.75 mmol) was added to a mixture of NaOAc (4 g) in Ac_2O (40 mL) and heated to 130 °C for 12 h. A drying tube was attached to the reaction vessel and the mixture was allowed to cool slowly to room temperature. The acetic anhydride was removed under vacuum and the remaining residues were partitioned between $CHCl_3$ and H_2O. The aqueous layer was extracted with $CHCl_3$ (5 × 50 mL) and the combined organic layers washed with H_2O (5 × 100 mL). The organic layers were dried over Na_2SO_4 (anhyd.) and the solvent removed under reduced pressure. The residues were dried under vacuum overnight. The product was purified by flash column chromatography (silica), eluting with EtOAc–hexane (1 : 1) to obtain a light cream coloured solid (810 mg, 81%); mp 232–234 °C; ^{1}H NMR ($CDCl_3$) δ 7.42 (2H, m, Ar), 6.94 (2H, m, Ar), 6.74 (4H, m), 5.34 (4H, m), 1.29 (9H, s); ^{13}C NMR ($CDCl_3$) δ 173.4, 152.1, 139.2, 128.4, 126.2, 125.4, 81.6, 69.1, 34.7, 31.2; HRMS $C_{22}H_{21}NO_4$: calculated 363.1471; *m/z* (EI) M$^+$ observed 363.1482.

Method 2. The amic acid **3a** (15 mg, 3.9 × 10^{-5} mol) and *N*-hydroxybenzotriazole (HOBT, 8 mg, 6 × 10^{-5} mol) were dissolved in dry tetrahydrofuran (THF, 1.5 mL) and stirred for 5 min under N_2 (g). *N*-(3-dimethylaminopropyl)-*N*′-ethylcarbodiimide hydrochloride (EDC, 11 mg, 6 × 10^{-5} mol) and Et_3N (dry, 50 μL) were added in quick succession (under N_2) and the mixture was stirred at room temperature under N_2 for 3 d. THF was removed under vacuum and the residues partitioned between $CHCl_3$ (*ca.* 3 mL) and 6M $HCl_{(aq)}$ (*ca.* 2 mL). The aqueous layer was neutralised with $NaHCO_3$ (aq sat.) and extracted with $CHCl_3$. The combined organics were washed with water (3 × 5 mL), dried over $NaSO_4$ (anhyd.) and concentrated using a rotary evaporator. The residues were dissolved in a minimum of CH_2Cl_2 and precipitation of the product was induced by the slow addition of hexane to this solution. The fine white solid was filtered and dried under vacuum to give a white powder (12 mg, 80%). Both the melting point and ^{1}H NMR data were identical to results obtained from method 1 above.

1α,2β,3α,6α,7β,8α-*N*-(4-methoxyphenyl)-11,12-dioxatetracyclo-[6.2.1.1^{3,6}.0^{2,7}]dodeca-4,9-dien-2,7-dicarboximide (4b).

Method 1. A mixture of the anhydride of (**1**) (526 mg, 2.27 mmol) and anisidine (286 mg, 2.32 mmol) in CH_2Cl_2 (4.5 mL) were placed under high pressure (13 kbar) for 3 d. The solvent was removed under reduced pressure and the residues dried under vacuum. The crude residue was treated with NaOAc (1 g) in Ac_2O (5 mL) and this mixture was stirred at room temperature for 2 d and then at 60 °C for 1 d. The acetic anhydride was removed under high vacuum and the residues were partitioned between $CHCl_3$ and H_2O. The aqueous layer was extracted with $CHCl_3$ (3 × 50 mL) and the combined organic layers washed with H_2O (3 × 100 smL). The organic layers were dried over Na_2SO_4 (anhyd.) and the solvent removed under reduced pressure. The remaining residue was dried under vacuum overnight. The product was recrystallised from EtOAc–hexane (2 : 1) giving a fine off-white solid (360 mg, 47%); mp 275–278 °C; ^{1}H NMR ($CDCl_3$) δ 6.92 (4H, s, Ar), 6.74 (4H, m), 5.33 (4H, m), 3.79 (3H, s).

Method 2. The amic acid **3b** (50 mg, 1.41 × 10^{-4} mol) was stirred with NaOAc (300 mg) in Ac_2O (3 mL) at 130 °C for 3 h. The acetic anhydride was distilled off under vacuum and the remaining residues were partitioned between $CHCl_3$ and H_2O. The organic layer was separated and the aqueous layer extracted with $CHCl_3$ (4 × 5 mL). The combined organics were washed with water (4 × 5 mL), dried over $NaSO_4$ (anhyd.) and the solvent removed using a rotary evaporator. The residue was dissolved in a minimum of $CHCl_3$ (*ca.* 2 mL) and approximately 1 mL of hexane was added down the side of the flask. A fine white precipitate formed and was filtered and dried under vacuum overnight (40 mg, 84%). Both the melting point and NMR data were identical to results obtained from method 1 above.

Method 3. The amic acid **3b** (21 mg, 5.8 × 10^{-5} mol) and HOBT (12 mg, 8.8 × 10^{-5} mol) were dissolved in dry THF (2 mL) and stirred for 5 min under N_2 (g). EDC (17 mg, 8.8 × 10^{-5} mol) and Et_3N (dry, 70 μL) were added in quick succession and the mixture stirred at room temperature under N_2 (g) for 3 d. THF was removed under vacuum and the residues partitioned between $CHCl_3$ (*ca.* 3 mL) and 6M HCl (aq, *ca.* 2 mL). The aqueous layer was neutralised with $NaHCO_3$ (aq sat.) and extracted with $CHCl_3$. The combined organics were washed with water (3 × 5 mL), dried over $NaSO_4$ (anhyd.) and concentrated using a rotary evaporator. The residues were dissolved in a minimum of CH_2Cl_2 and precipitation of the product was induced by the slow addition of hexane to this solution. A fine white solid was filtered off and dried under vacuum to give a white powder (13.7 mg). Yield = 70%. Both the melting point and ^{1}H NMR data were identical to results obtained from method 1 above.

1α,2β,3α,6α,7β,8α-*N*-(4-methylphenyl)-11,12-dioxatetracyclo-[6.2.1.1^{3,6}.0^{2,7}]dodeca-4,9-dien-2,7-dicarboximide (4c). The amic acid **3c** (20 mg, 5.9 × 10^{-5} mol) and HOBT (12 mg, 8.8 × 10^{-5} mol) were dissolved in dry THF (2 mL) and stirred for 5 min under N_2 (g). EDC (17 mg, 8.8 × 10^{-5} mol) and Et_3N (dry, 70 μL) were added in quick succession and the mixture stirred at room temperature under N_2 (g) for 3 d. THF was removed under vacuum and the residues partitioned between $CHCl_3$ (*ca.* 3 mL) and 6M $HCl_{(aq)}$ (*ca.* 2 mL). The aqueous layer was neutralised with $NaHCO_3$ (aq sat.) and extracted with $CHCl_3$. The combined organics were washed with water (3 × 5 mL), dried over $NaSO_4$ (anhyd.) and concentrated using a rotary evaporator. The residues were dissolved in a minimum of CH_2Cl_2 and precipitation of the product was induced by the slow addition of hexane to this solution. The fine white solid was filtered and dried under vacuum to give a white powder (10 mg, 50%); mp 270–273 °C; ^{1}H NMR ($CDCl_3$) δ 7.21 (2H, m, Ar), 6.88 (2H, m, Ar), 6.75 (4H, bs), 5.34 (4H, bs), 2.35 (3H, s); HRMS $C_{19}H_{15}NO_4$: calculated 321.1001; *m/z* (EI) M$^+$ 321.1002.

1α,2β,3α,6α,7β,8α-*N*-(4-chlorophenyl)-11,12-dioxatetracyclo-[6.2.1.1^{3,6}.0^{2,7}]dodeca-4,9-dien-2,7-dicarboximide (4d). The amic acid **3d** (50 mg, 1.4 × 10^{-4} mol) and HOBT (28 mg, 2.1 × 10^{-4} mol) were dissolved in dry THF (4 mL) and stirred for 5 min under N_2 (g). EDC (40 mg, 2.1 × 10 $^{-4}$ mol) and Et_3N (dry, 160 μL) were added in quick succession and the mixture stirred at room temperature under N_2 (g) for 3 d. THF was removed under vacuum and the residues partitioned between $CHCl_3$ (*ca.* 5 mL)

and 6M $HCl_{(aq)}$ (*ca.* 5 mL). The aqueous layer was neutralised with $NaHCO_3$ (aq sat.) and extracted with $CHCl_3$. The combined organics were washed with water (3 × 10 mL), dried over $NaSO_4$ (anhyd.) and concentrated using a rotary evaporator. The residues were dissolved in a minimum of CH_2Cl_2 and precipitation of the product was induced by the slow addition of hexane to this solution. The white precipitate was filtered and dried under vacuum to give a white powder (30 mg, 63%); mp 263–266 °C; ^{1}H NMR ($CDCl_3$) δ 7.39 (2H, m, Ar), 6.97 (2H, m, Ar), 6.75 (4H, s), 5.34 (4H, s); HRMS $C_{18}H_{12}ClNO_4$: calculated 341.0455; *m/z* (EI) M^+ observed 341.0453.

(1α,2β,3α,4β,7β,8α,9β,10α,11β,14β)-*N*-(4-*tert*-butylphenyl)-5,6,12,13-tetra(methoxycarbonyl)-15,16-dioxahexacyclo[8.4.1.1^{3,8}·0^{2,9}·0^{4,7}·0^{11,14}]hexadeca-5,12-diene-2,9-dicarboximide (5a). To a solution of **4a** (85.3 mg, 2.35 × 10^{-4} mol) and DMAD (190 mg, 1.34 mmol, 5.7 eqv.) in benzene (5 mL) was added $RuH_2CO(PPh_3)_3$ (10 mol%, 21 mg). The solution was heated at reflux temperature under N_2 for 3 d. The solution was taken to dryness (rotary evaporator) and the residue dissolved in EtOAc. Solids were filtered off and washed well with EtOAc. The filtrate was concentrated and the product recrystallised from EtOAc–hexane to give a white solid (84 mg, 55%); mp 284–286 °C; ^{1}H NMR ($CDCl_3$) δ 7.49 (2H, m, Ar), 7.10 (2H, m, Ar), 4.84 (4H, s), 3.79 (12H, s), 3.26 (4H, s), 1.32 (9H, s); ^{13}C NMR ($CDCl_3$) δ 171.9, 160.0, 152.8, 140.1, 127.9, 126.5, 125.5, 77.2 (hidden), 70.2, 52.2, 44.8, 34.9, 31.2; HRMS $C_{34}H_{33}NO_{12}$: calculated 647.2003; *m/z* (EI) M^+ observed 647.1998.

(1α,2β,3α,4β,7β,8α,9β,10α,11β,14β)-*N*-(4-methoxyphenyl)-5,6,12,13-tetra(methoxycarbonyl)-15,16-dioxahexacyclo[8.4.1.1^{3,8}·0^{2,9}·0^{4,7}·0^{11,14}]hexadeca-5,12-diene-2,9-dicarboximide (5b). To a solution of **4b** (200 mg, 5.93 × 10^{-4} mol) and DMAD (211 mg, 1.48 mmol, 2.5 eqv.) in benzene (8 mL) was added $RuH_2CO(PPh_3)_3$ (2 mol%, 11 mg). The solution was heated at reflux temperature under N_2 (g) for 2 d. The solution was taken to dryness (rotary evaporator) and the residue dissolved in EtOAc. Solids were filtered off and washed well with EtOAc. The filtrate was concentrated and the residue purified by flash column chromatography (silica, EtOAc–hexane 1 : 1) giving a white solid (111 mg, 30%); mp 248–250 °C; ^{1}H NMR ($CDCl_3$) δ 7.49 (2H, m, Ar), 7.10 (2H, m, Ar), 4.84 (4H, s), 3.79 (12H, s), 3.26 (4H, s), 1.32 (9H, s); HRMS $C_{31}H_{27}NO_{13}$: calculated 621.1482; *m/z* (EI) M^+ observed 621.1487.

(1α,2β,3α,4β,5α,7α,8β,9α,10β,11α,12β,13α,15α,16β)-*N*-(4-*tert*-butylphenyl)-5,7,13,15-tetra(methoxycarbonyl)-6,14,17,18-tetraoxaoctacyclo[9.5.1.1^{3,9}·0^{2,10}·0^{4,8}·0^{5,7}·0^{12,16}·0^{13,15}]octadeca-2,9-dicarboximide (6a). The *bis*-cyclobutenediester **5a** (88 mg, 1.30 × 10^{-4} mol) was dissolved in dry THF (7 mL) and cooled to −8 °C. ^{t}BuOOH (3.8 M in toluene, 89 μL, 3.4 × 10^{-4} mol, *ca.* 1.3 eqv. per 'ene' group) was added and the solution stirred at −5 °C for 10 min. ^{t}BuOK (14.6 mg, 1.30 × 10^{-4} mol, 0.5 eqv. per 'ene' group) was added under N_2 and the reaction mixture was stirred and allowed to rise gradually to +25 °C over several hours. Stirring under N_2 at *ca.* 25 °C was continued overnight. An aqueous solution of Na_2SO_3 (10% *w/v*, 7 mL) was added with $CHCl_3$ (7 mL) and the mixture stirred for 5 min. The organic layer was separated and the aqueous layer extracted with $CHCl_3$ (3 × 7 mL). The combined organics were washed with water (3 × 20 mL), dried over Na_2SO_4 (anhyd.) and the solvents removed using a rotary evaporator. The residue was dried under vacuum giving an off-white solid. The product was purified by flash column chromatography (silica, $CHCl_3$) and obtained as a white solid (68 mg, 74%); mp > 300 °C (sample changes colour and gradually liquifies at T > 150 °C); ^{1}H NMR ($CDCl_3$) δ 7.47 (2H, m, Ar), 6.99 (2H, m, Ar), 5.58 (4H, s), 3.83 (12H, s), 2.90 (4H, s), 1.31 (9H, s); ^{13}C NMR ($CDCl_3$) δ 171.4, 163.2, 152.9, 127.6, 126.6, 125.4, 80.6, 70.4, 62.7, 53.1, 48.7, 34.8, 31.2; HRMS $C_{34}H_{33}NO_{14}$: calculated 679.1901; *m/z* (EI) M^+ observed 679.1889.

(1α,2β,3α,4β,5α,7α,8β,9α,10β,11α,12β,13α,15α,16β)-*N*-(4-methoxyphenyl)-5,7,13,15-tetra(methoxycarbonyl)-6,14,17,18-tetraoxaoctacyclo[9.5.1.1^{3,9}·0^{2,10}·0^{4,8}·0^{5,7}·0^{12,16}·0^{13,15}] octadeca-2,9-dicarboximide (6b). The *bis*-cyclobutenediester **5b** (80 mg, 1.29 × 10^{-4} mol) was dissolved in dry THF (5 mL) and cooled to −78 °C (dry ice–acetone). ^{t}BuOOH (3.8 M in toluene, 110 μL, 4.2 × 10^{-4} mol, *ca.* 1.3 eqv. per 'ene' group) was added and the solution stirred at −78 °C for 10 min. MeLi (1.4 M, 0.278 mL) was added under N_2 and the reaction mixture was stirred at −78 °C for 30 min and allowed to rise gradually to rt over 2 h. Stirring under N_2 at rt was continued for another 6 h. The reaction mixture was diluted with CH_2Cl_2 (50 mL) and washed with Na_2SO_3 (aq) (10% *w/v*, 2 × 50 mL), water (3 × 20 mL) and dried over Na_2SO_4 (anhyd). The solvents were removed using a rotary evaporator and the residue was dried under vacuum giving a white solid. The product was further purified by flash column chromatography (silica, $CHCl_3$) and obtained as a white solid (63 mg, 75%); mp > 250 °C; ^{1}H NMR ($CDCl_3$) δ 6.96 (4H, s), 5.57 (4H, s), 3.83 (12H, s), 3.81 (3H, s), 2.90 (4H, s).

^{t}BuPSP 10a. In a thick-walled glass reaction tube a solution of ^{t}BuPBlock **9** (111 mg, 8.16 × 10^{-5} mol) and *bis*-epoxide **6a** (28 mg, 4.1 × 10^{-5} mol) in CH_2Cl_2 (3.0 mL) was degassed, by freeze-thawing (×4) under high vacuum. The reaction vessel was flame-sealed under vacuum and the solution heated and magnetically stirred at 140 °C for 90 h. The reaction mixture was added directly to the top of a wet (2% MeOH–CH_2Cl_2) silica column and the product purified chromatographically (flash column). The product was obtained as a brown solid (80 mg) and further purified by recrystallisation from CH_2Cl_2–MeOH gave the final product (52 mg, 38%). Mp > 300 °C; ^{1}H NMR ($CDCl_3$) δ 9.02 (4H, d, J = 5 Hz), 8.97 (4H, d, J = 5 Hz), 8.77 (4H, s), 8.50 (4H, s), 8.10 (8H, s), 7.99 (4H, s), 7.95 (4H, s), 7.81 (4H, s), 7.30 (2H, m), 6.95 (2H, m), 6.55 (4H, t, J = 4 Hz), 4.72 (4H, s), 4.26 (4H, t, J = 4 Hz), 3.96 (12H, s), 2.46 (4H, s), 2.39 (4H, s), 2.20 (2H, d, J = 10 Hz), 2.06 (2H, d, J = 10 Hz), 1.92 (4H, s), 1.90 (4H, s), 1.53 (36H, s), 1.52 (36H, s), 1.49 (72H, s), 0.98 (3H, s) −2.40 (4H, bs); ^{13}C NMR ($CDCl_3$) δ 172.0, 168.1, 158.5, 155.0, 153.7, 149.1, 149.0, 148.8, 145.5, 141.0, 140.7, 139.8, 139.6, 138.9, 138.1, 134.2, 133.6, 129.5, 129.0, 128.6, 128.3, 128.1, 126.5, 124.9, 123.0, 121.2, 120.7, 117.9, 89.5, 82.7, 70.6, 57.2, 52.9, 52.8, 46.7, 46.5, 43.8, 35.0, 35.0, 31.9, 31.7, 30.9.

Zn_2^{t}BuPSP 10b. To a refluxing solution of ^{t}BuPSP **10a** (12.0 mg, 3.53 μmol) in $CHCl_3$ (500 μL) was added a saturated solution of zinc acetate dihydrate in MeOH (150 μL). The mixture was heated at reflux temperature for 30 min. The reaction mixture was partitioned between $CHCl_3$ and H_2O. The organic layer was separated and the aqueous layer extracted with $CHCl_3$. The

combined organic layers were washed with H_2O (3 × 10 mL), dried over Na_2SO_4 (anhyd.) and the solvent removed under reduced pressure. The product was recrystallised from $CHCl_3$–MeOH giving the product **10b** as a brown solid (11.1 mg, 90%); m.p. > 300 °C; ^{1}H NMR ($CDCl_3$) δ 8.94 (8H, s), 8.84 (4H, s), 8.56 (4H, s), 8.06 (8H, bs), 7.95 (8H, bs), 7.92 (4H, bs), 7.27 (2H, m), 6.93 (2H, m), 6.54 (4H, t, J = 4 Hz), 4.70 (4H, s), 4.25 (4H, bs), 3.94 (12H, s), 2.44 (4H, s), 2.38 (4H, s), 2.19 (2H, d, J = 10 Hz), 2.04 (2H, d, J = 10 Hz), 1.92 (4H, s), 1.88 (4H, s), 1.52 (36H, s), 1.51 (36H, s), 1.47 (72H, s), 0.96 (3H, s); HRMS $C_{224}H_{241}N_{17}O_{14}Zn_2$: calculated 3522.741; m/z (ES) $(M + 2H)^{2+}$ observed 1761.369.

Nicotinic acid 5-nicotinoyloxy-naphthalen-1-yl ester (11a). To naphthalene-1,5-diol (160 mg, 1.0 mmol), nicotinic acid (369 mg, 3.0 mmol) and HOBT (405 mg, 3.0 mmol) in dry THF (20 mL) under N_2 was added EDC (575 mg, 3.0 mmol) followed by Et_3N (dry, 800 μL). The solution was stirred under N_2 at rt in darkness for 5 d. The solvents were removed under reduced pressure and the residue was partitioned between $CHCl_3$ and H_2O. The aqueous layer was extracted with $CHCl_3$ and the combined organics washed with water, dried over $NaSO_4$ (anhyd.) and the solvent removed on a rotary evaporator. The product was dried under vacuum overnight giving a reddish-brown solid (320 mg, 87%); mp 189–192 °C; ^{1}H NMR ($CDCl_3$) δ 9.55 (2H, s), 8.92 (2H, d, J = 4 Hz), 8.57 (2H, m), 7.89 (2H, d, J = 8 Hz), 7.59–7.51 (4H, m), 7.46 (2H, d, J = 8 Hz); HRMS $C_{22}H_{14}N_2O_4$: calculated 370.0954; m/z (EI) M^+ observed 370.0952.

Nicotinic acid 2-[5-(2-nicotinoyloxyethoxy)naphthalen-1-yloxy]-ethyl ester (11b). A solution of 2-chloroethanol (3.2 g, 34 mmol) naphthalene-1,5-diol (1.6 g, 10 mmol) and K_2CO_3 (7 g) in MeCN (40 mL) was refluxed under N_2 for 7 d. The reaction mixture was allowed to cool to rt and the solids were filtered off and washed with $CHCl_3$ (30 mL). The filtrate was concentrated and the residues were partitioned between $CHCl_3$ and H_2O. The organic layer was washed with $NaHCO_3$ (aq sat.), dil. HCl (aq), and finally with H_2O. The organics were dried over Na_2SO_4 and the solvent removed using a rotary evaporator. The residues were dried under vacuum overnight. To a portion of this crude 1,5-*bis*-(2-hydroxyethoxy)naphthalen (355 mg, 1.43 mmol), nicotinic acid (1.0 g, 8.1 mmol) and HOBT (1.1 g, 8.1 mmol) in dry THF (24 mL) and $CHCl_3$ (12 mL) under N_2 was added EDC (1.2 g, 6.0 mmol) followed by Et_3N (dry, 830 μL). A white precipitate formed immediately upon the addition of triethylamine. The mixture was stirred under N_2 at rt in darkness for 3 d. The solvents were removed under reduced pressure and the residue was partitioned between $CHCl_3$ and HCl (aq) (6 M). The aqueous layer was neutralised and extracted with $CHCl_3$ and the combined organics washed with water and dried over $NaSO_4$ (anhyd.). The product was purified by recrystallisation from $CHCl_3$–hexane giving a light-red solid (400 mg, 60%); mp 128–130 °C; ^{1}H NMR (d_6-acetone) δ 9.17 (2H, d, J = 2Hz), 8.78 (2H, s), 8.35–8.31 (2H, m), 7.86 (2H, d, J = 8.5 Hz), 7.53–7.49 (2H, m), 7.37 (2H, t, J = 8 Hz), 7.05 (2H, d, J = 8 Hz), 4.88 (4H, t, J = 5 Hz), 4.59 (4H, t, J = 5 Hz); HRMS $C_{26}H_{22}N_2O_6$: calculated 458.1478; m/z (M^+) EI observed 458.1471.

Nicotinic acid 3-[5-(3-nicotinoyloxypropoxy)naphthalen-1-yloxy]-propyl ester (11c). In a similar procedure to that for **11a**, but using 3-bromopropan-1-ol (5.6 g, 40 mmol) was obtained crude 1,5-*bis*-(3-hydroxy-propoxy)naphthalene. This product (204 mg, 0.74 mmol) was reacted with nicotinic acid (0.37 g, 3.0 mmol), HOBT (0.40 g, 3.0 mmol), EDC (0.43 g, 2.2 mmol) and Et_3N (dry, 500 μL) in dry THF (15 mL) and $CHCl_3$ (5 mL) under N_2 as above giving the product as a pink solid (228 mg, 64%); mp 151–153 °C; ^{1}H NMR ($CDCl_3$) δ 9.22 (2H, m), 8.76 (2H, s), 8.29–8.25 (2H, m), 7.86 (2H, d, J = 8 Hz), 7.38–7.30 (4H, m), 6.85 (2H, d, J = 7.3 Hz), 4.67 (4H, t, J = 6 Hz), 4.30 (4H, t, J = 6 Hz), 2.41 (4H, t, J = 6 Hz); HRMS $C_{28}H_{26}N_2O_6$: calculated 486.1791; m/z (M^+) EI observed 486.1786.

Nicotinic acid 4-[5-(4-nicotinoyloxybutoxy)naphthalen-1-yloxy]-butyl ester (11d). In a similar procedure to that for **11a**, but using 4-chlorobutan-1-ol (85% tech. grade, 5.0 g, 28 mmol) was obtained crude *bis*-(hydroxybutoxy)naphthalene. This product (700 mg, 2.3 mmol) was reacted with nicotinic acid (1.2 g, 9.7 mmol), HOBT (1.30 g, 9.7 mmol), EDC (1.15 g, 6.0 mmol) and Et_3N (dry, 1.00 mL) in dry THF (24 mL) and $CHCl_3$ (12 mL) under N_2 as above giving the product as a thick red oil (600 mg, 60%) of the pure product (red oil) was obtained by preparative TLC (alumina, $CHCl_3$–EtOAc 9 : 1); ^{1}H NMR ($CDCl_3$) δ 9.22 (2H, d, 2 Hz), 8.75 (2H, s), 8.28–8.24 (2H, m), 7.82 (2H, d, J = 8.5 Hz), 7.37–7.30 (4H, m), 6.82 (2H, d, J = 7.6 Hz), 4.49 (4H, t, J = 6 Hz), 4.20 (4H, t, J = 6 Hz), 2.09 (8H, m); HRMS $C_{30}H_{30}N_2O_6$: calculated 514.2104; m/z (M^+) EI observed 514.2107.

Nicotinic acid 6-[5-(6-nicotinoyloxyhexoxy)naphthalen-1-yloxy]-hexyl ester 11e. In a similar procedure to that for **11a**, but using 6-bromohexan-1-ol (5.0 g, 28 mmol) was obtained crude 1,5-*bis*-(6-hydroxy-hexyloxy)naphthalene. This product (1.29 g, 3.58 mmol) was reacted with nicotinic acid (1.76 g, 14.3 mmol), HOBT (1.93 g, 4.3 mmol), EDC (2.05 g, 10.74 mmol) and Et_3N (dry, 2.00 mL) in dry THF (40 mL) and $CHCl_3$ (20 mL) under N_2 as above giving the product as a red sticky oil (1.4 g, 69%); ^{1}H NMR ($CDCl_3$) δ 9.20 (2H, bs), 8.75 (2H, bs), 8.31–8.24 (2H, m), 7.82 (2H, d, J = 8.5 Hz), 7.40–7.29 (4H, m), 6.80 (2H, d, J = 7.6 Hz), 4.39 (4H, t, J = 6 Hz), 4.11 (4H, t, J = 6 Hz), 1.99–1.89 (8H, m), 1.68–1.56 (8H, m); HRMS $C_{34}H_{38}N_2O_6$: calculated 570.2730; m/z (M^+) EI observed 570.2730.

***bis*-[2-(4-Pyridyl)-1*H*-imidazo]porphyrin (13).** 2,3,12,13-Tetra-oxo-5,10,15,20-*tetrakis*-(3,5-di-*tert*-butylphenyl)porphyrin (26 mg, 2.3×10^{-5} mol), pyridine-4-carbaldehyde (6.5 mg, 6.0×10^{-5} mol) and NH_4OAc (50 mg) were stirred in refluxing AcOH (glacial)–$CHCl_3$ (1 : 1, 5 mL) for 4 h. The reaction mixture was washed with water (3 × 10 mL), $NaHCO_3$ (aq) (3 × 10 mL) and again with water (2 × 10 mL), dried over $NaSO_4$ (anhyd.) and the solvent removed using a rotary evaporator. The residue was purified using flash column chromatography (silica, $CHCl_3$) giving **13** (10 mg, 34%); mp > 300 °C; ^{1}H NMR ($CDCl_3$) broad unresolved spectrum; UV-Vis (CH_2Cl_2) λ_{max} (log ε)/nm 423 (5.15), 516 (4.03), 551 (3.93), 587 (3.87), 638 (3.54), 659 (3.53); HRMS $C_{88}H_{100}N_{10}$: calculated 1297.821; m/z (ES) $(M + H)^+$ observed 1297.820

Acknowledgements

We thank the Australian Research Council (ARC) for financial support for part of this work.

References

1 J.-M. Lehn, *Angew. Chem., Int. Ed. Engl.*, 1988, **27**, 89; V. Balzani and F. Scandola, in *Comprehensive Supramolecular Chemistry, Vol. 10*, ed. D. N. Reinhoudt, Pergamon Press, Oxford, England, 1996, pp. 687–746.
2 V. Balzani, A. Credi and M. Venturi, *Chem. Eur. J.*, 2002, **8**, 5525.
3 V. Balzani, M. Gómez-Lopez and J. F. Stoddart, *Acc. Chem. Res.*, 1998, **31**, 405; V. Balzani, A. Credi, F. M. Raymo and J. F. Stoddart, *Angew. Chem., Int. Ed.*, 2000, **39**, 3349; F. M. Raymo and J. F. Stoddart, in *Supramolecular Organisation and Materials Design*, ed. W. Jones and C. N. R. Rao, Cambridge University Press, Cambridge, UK, 2002, pp. 332–362; J. F. Stoddart, *Acc. Chem. Res.*, 2001, **34**, 410; R. Ballardini, V. Balzani, A. Credi, M. T. Gandolfi and M. Venturi, *Acc. Chem. Res.*, 2001, **34**, 445.
4 B. L. Feringa, *Acc. Chem. Res.*, 2001, **34**, 504.
5 W. Abraham, L. Grubert, U. W. Grummt and K. Buck, *Chem. Eur. J.*, 2004, **10**, 3562; R. Ballardini, V. Balzani, A. Credi, M. T. Gandolfi and M. Venturi, *Struct. Bonding*, 2001, **99**, 163; V. Balzani, A. Credi, S. J. Langford, F. M. Raymo, J. F. Stoddart and M. Venturi, *J. Am. Chem. Soc.*, 2000, **122**, 3542; C. J. Easton, S. F. Lincoln, L. Barr and H. Onagi, *Chem. Eur. J.*, 2004, **10**, 3120; K.-S. Jeong, K.-J. Chang and Y.-J. An, *Chem. Commun.*, 2003, 1450.
6 M. Liu, D. H. Waldeck, A. M. Oliver, N. J. Head and M. N. Paddon-Row, *J. Am. Chem. Soc.*, 2004, **126**, 10778; M. N. Paddon-Row, in *Advances in Physical Organic Chemistry, Vol. 38*, 2003, pp. 1–85; N. R. Lokan, M. N. Paddon-Row, M. Koeberg and J. W. Verhoeven, *J. Am. Chem. Soc.*, 2000, **122**, 5075.
7 A. M. Napper, N. J. Head, A. M. Oliver, M. J. Shephard, M. N. Paddon-Row, I. Read and D. H. Waldeck, *J. Am. Chem. Soc.*, 2002, **124**, 10171; A. M. Napper, I. Read, D. H. Waldeck, N. J. Head, A. M. Oliver and M. N. Paddon-Row, *J. Am. Chem. Soc.*, 2000, **122**, 5220.
8 M. R. Johnston, M. J. Latter and R. N. Warrener, *Aust. J. Chem.*, 2001, **54**, 633.
9 M. R. Johnston, M. J. Latter and R. N. Warrener, *Org. Lett.*, 2002, **4**, 2165.
10 M. R. Johnston, M. J. Gunter and R. N. Warrener, *Chem. Commun.*, 1998, 2739.
11 L. Flamigni, A. M. Talarico, F. Barigelletti and M. R. Johnston, *Photochem. Photobiol. Sci.*, 2002, **1**, 190.
12 L. Flamigni and M. R. Johnston, *New J. Chem.*, 2001, **25**, 1368.
13 L. Flamigni, M. R. Johnston and L. Giribabu, *Chem. Eur. J.*, 2002, **8**, 3938.
14 R. N. Warrener, H. S. Suna and M. R. Johnston, *Aust. J. Chem.*, 2003, **56**, 269.
15 M. R. Johnston, *Molecules*, 2001, **6**, 406.
16 L. Flamigni, G. Marconi and M. R. Johnston, *Phys. Chem. Chem. Phys.*, 2001, **3**, 4488.
17 M. J. Shephard and M. N. Paddon-Row, *J. Phys. Chem. A*, 2000, **104**, 11628.
18 N. J. Head, A. M. Oliver, K. Look, N. R. Lokan, G. A. Jones and M. N. Paddon-Row, *Angew. Chem., Int. Ed.*, 1999, **38**, 3219.
19 R. N. Warrener, A. C. Schultz, D. N. Butler, S. Wang, I. B. Mahadevan and R. A. Russell, *Chem. Commun.*, 1997, 1023.
20 R. N. Warrener, S. Wang and R. A. Russell, *Tetrahedron*, 1997, **53**, 3975; R. N. Warrener, A. C. Schultz, M. A. Houghton and D. N. Butler, *Tetrahedron*, 1997, **53**, 3991; R. N. Warrener, G. Abbenante and C. H. L. Kennard, *J. Am. Chem. Soc.*, 1994, **116**, 3645.
21 G. Maier and W. A. Jung, *Chem. Ber.*, 1982, **115**, 804.
22 T. Mitsudo, K. Kokuryo, T. Shinsugi, Y. Nakagawa, Y. Watanabe and Y. Takegami, *J. Org. Chem.*, 1979, **44**, 4492.
23 J. J. Levison and S. D. Robinson, *J. Chem. Soc. A*, 1970, 2947.
24 R. N. Warrener, D. N. Butler, D. Margetic, F. M. Pfeffer and R. A. Russell, *Tetrahedron Lett.*, 2000, **41**, 4671.
25 M. J. Crossley, P. L. Burn, S. S. Chew, F. B. Cuttance and I. A. Newsom, *J. Chem. Soc., Chem. Commun.*, 1991, 1564; M. J. Crossley and P. L. Burn, *J. Chem. Soc., Chem. Commun.*, 1991, 1569; M. J. Crossley, P. L. Burn, S. J. Langford, S. M. Pyke and A. G. Stark, *J. Chem. Soc., Chem. Commun.*, 1991, 1567; M. J. Crossley, L. J. Govenlock and J. K. Prashar, *J. Chem. Soc., Chem. Commun.*, 1995, 2379.
26 R. N. Warrener, M. R. Johnston and M. J. Gunter, *SYNLETT*, 1998, **6**, 593.
27 A. C. Schultz, M. R. Johnston, R. N. Warrener and M. J. Gunter, in *Electronic Conference on Heterocyclic Chemistry '98*, ed. H. S. Rzepa and O. Kappe, Imperial College Press, 1998; R. N. Warrener, A. C. Schultz, M. R. Johnston and M. J. Gunter, *J. Org. Chem.*, 1999, **64**, 4218.
28 M. R. Johnston, M. J. Gunter and R. N. Warrener, *Tetrahedron*, 2002, **58**, 3445.
29 H. L. Anderson, S. Anderson and J. K. M. Sanders, *J. Chem. Soc., Perkin Trans. 1*, 1995, 2231.
30 H. L. Anderson, C. A. Hunter, M. N. Meah and J. K. M. Sanders, *J. Am. Chem. Soc.*, 1990, **112**, 5780; S. Anderson, H. L. Anderson and J. K. M. Sanders, *Acc. Chem. Res.*, 1993, **26**, 469; C. A. Hunter, M. N. Meah and J. K. M. Sanders, *J. Chem. Soc., Chem. Commun.*, 1988, 694; C. A. Hunter, P. Leighton and J. K. M. Sanders, *J. Chem. Soc., Perkin Trans. 1*, 1989, 547; R. S. Wylie, E. G. Levy and J. K. M. Sanders, *Chem. Commun.*, 1997, 1611.
31 M. Nakash and J. K. M. Sanders, *J. Org. Chem.*, 2000, **65**, 7266; J. K. M. Sanders, *Chem. Eur. J.*, 1998, **4**, 1378; M. Nakash, Z. Clyde-Watson, N. Feeder, J. E. Davies, S. J. Teat and J. K. M. Sanders, *J. Am. Chem. Soc.*, 2000, **122**, 5286; Z. Clyde-Watson, A. Vidal-Ferran, L. J. Twyman, C. J. Walter, D. W. J. McCallien, S. Fanni, N. Bampos, R. S. Wylie and J. K. M. Sanders, *New J. Chem.*, 1998, **22**, 493.
32 M. J. Crossley and P. Thordarson, *Angew. Chem., Int. Ed.*, 2002, **41**, 1709; P. Thordarson, A. Marquis and M. J. Crossley, *Org. Biomol. Chem.*, 2003, **1**, 1216.
33 J. K. M. Sanders, N. Bampos, Z. Clyde-Watson, S. L. Darling, J. C. Hawley, H.-J. Kim, C. C. Mak and S. J. Webb, in *The Porphyrin Handbook, Vol. 3, Ch. 15*, ed. K. M. Kadish, K. M. Smith and R. Guilard, Academic Press, New York, 2000, p. 1.
34 M. J. Crossley and J. A. McDonald, *J. Chem. Soc., Perkin Trans. 1*, 1999, **1**, 2429.
35 U. Michelsen and C. A. Hunter, *Angew. Chem., Int. Ed.*, 2000, **39**, 764; K. S. Cameron and L. Fielding, *J. Org. Chem.*, 2001, **66**, 6891; L. Frish, M. O. Vysotsky, S. E. Matthews, V. Bohmer and Y. J. Cohen, *J. Chem. Soc., Perkin Trans. 2*, 2002, 88.
36 M. R. Johnston and M. J. Latter, *J. Porphyrins Phthalocyanines*, 2002, **6**, 798.
37 R. Kersserbaum, *DOSY and Diffusion by NMR: Users Guide for XWinNMR 3.1 Preliminary Version 0.99*, Bruker; Bruker BioSpin GmbH, Rheinstetten, Germany, 2002.

